THE JOURNAL OF PHYSICAL CHEMISTRY A
A JOURNAL OF THE AMERICAN CHEMICAL SOCIETY

pubs.acs.org/JPCA

Article

Spodium Bonding to Dicoordinated Group 12 Atoms

Akhtam Amonov and Steve Scheiner*

Cite This: *J. Phys. Chem. A* 2024, 128, 8751−8761

Read Online

ACCESS | Metrics & More | Article Recommendations | Supporting Information

ABSTRACT: DFT calculations consider the interactions between linear MR_2 and a series of N-bases, where M is Hg or Zn and its R substituents are CCH, CN, or NO_2. NCH, NH_3, and NMe_3 were considered as three different N-bases. Zn forms stronger bonds with the N bases than does Hg, and they strengthen along with the electron-withdrawing power of the R substituent, varying over a wide range from 3.4 to 43.9 kcal/mol. Another factor contributing to the bond strength is the nucleophilicity of the base: NCH < NH_3 < NMe_3. All MR_2 Lewis acids can bind at least two bases, which are situated along the R-M-R bisecting plane, fairly close to one another, with θ(N-M-N) angles between 67° and 117°. The presence of a more electron-withdrawing substituent R and more powerful nucleophile allows up to 4 bases to bind to M. The properties of these bonds place them along a continuum, some clearly noncovalent, while other contain a good deal of covalent character.

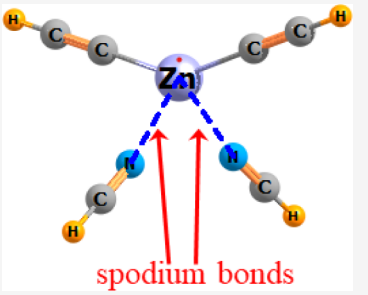

INTRODUCTION

The H-bond is arguably the most important of all noncovalent interactions, figuring prominently in a diverse range of chemical and biological phenomena such as solvation, genetic replication, and enzymatic activity.[1−9] Recent years have brought to the fore a class of closely related noncovalent bonds wherein the bridging proton is replaced by any of a large set of other atoms, mainly drawn from the right side of the periodic table.[10−17] Although these interactions do not have the advantage of a positive H atom to attract a nucleophile, they rely instead on a restricted region of positive electrostatic potential that lies along the extension of the covalent bond which connects this bridging atom to the Lewis acid molecule. This region of positive charge, attributed to a deficiency of electron density, has been termed a σ-hole and thus the associated bonds are classified as σ-hole bonds. In a more general sense, there are situations where the positive region lies not along a bond axis, but rather above the plane of the molecule, and is thus referred to as a π-hole.

It is common to subclassify these bonds according to the family of the periodic table from which the bridging atom is derived, thus leading to the halogen, chalcogen, pnicogen, tetrel, and triel bonds that have found their way into common chemical parlance. Their importance is undeniable, as their strength is comparable to the H-bond, exceeding it in many instances. Like the H-bond, these bonds too are major players in widespread chemical phenomena such as catalysis, supramolecular structure, self-assembly, and ion transport.[18−25] Intensive study of these interactions in recent years has led to a great deal of information and insights concerning their fundamental nature, their strength, and the way in which they are modified by both the identity of the bridging atom and any of its substituents.

There is of course no reason that these bridging atoms must be limited to the p-block elements on the right side of the periodic table. One might conjecture that the transition metals of the d-block, with their greater electropositivity, ought to present σ and π-holes that are even more positive than the nonmetallic atoms to their right, and perhaps then stronger interactions with a nucleophile. And in fact, the recent literature has sprung to life with a rapidly increasing number of tentative observations of interactions that have all the markings of bonds of this sort. In the spirit of the p-block family, these bonds are often named after the particular column of the periodic table. Those involving Group 12 metals have been christened spodium bonds[26−33] and those including Group 11 go by the moniker of either regium or coinage metal bonds.[34−41] Osme bonds encompass Group 8,[42,43] matere bonds arise from Group 7,[44−48] wolfium bonds denote Group 6,[49,50] and erythronium bonds correspond to Group 5.[51]

It is to the spodium bonds formed by the Group 12 atoms that the current work is directed. Their s^2d^{10} electron configurations make them a particularly interesting set of atoms, especially with regard to their potential to present σ or π-holes when covalently bonded to various substituents. The term spodium bond was first coined several years ago for the noncovalent interactions in which a Group 12 atom serves as electron acceptor[33] where it was clearly differentiated from an ordinary coordinate covalent bond. These workers studied the σ-holes found in tetrahedral tetracoordinated monomers,

Received: August 14, 2024
Revised: September 17, 2024
Accepted: September 23, 2024
Published: September 28, 2024

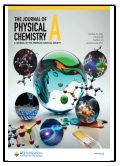

https://doi.org/10.1021/acs.jpca.4c05481
J. Phys. Chem. A 2024, 128, 8751−8761

which was soon followed by a number of other observations of such bonding patterns that included Hg[48,52,53] and Cd,[29,54−58] as well as Zn,[29,30,32,59] some in biological environments.[60,61] There has even been some examination of the idea of a spodium bond to an inert gas atom.[62]

A good deal of our understanding of the nature of this type of bond is derived from theoretical studies that can elucidate its interaction energy, as well as analyze the electronic structure that underpins the forces that hold it together. To this point, most calculations have been devoted to crystal structures, either individually or through CSD surveys,[27,28,52,54,60,63−66] or concerned themselves with intramolecular spodium bonds whose geometry is dictated by steric issues within the molecule.[67] As such, these studies have not included the geometry optimizations that would be required to learn the preferred geometry of this bond in the absence of other intermolecular interactions and crystal packing forces. Nor are these calculations of frozen geometries able to determine the full extent of the bond energy possible within an optimized structure.

Some recent work has presented an opportunity to examine the essential qualities of spodium bonding without risk of steric hindrance. Building on prior findings that disubstituted Hg, as in $Hg(CF_3)_2$[68] or $Hg(C_6F_5)_2$[69] can engage with nucleophiles in what would appear to be a noncovalent binding fashion, Onn et al.[70] have very recently noted that the Hg center placed between a pair of alkynyl groups engages in an interaction with fluoride. The Hg··F distance of 2.69 Å is longer than would be expected for a covalent bond, with a similarly long pair of Hg··N distances to the two N atoms of phenanthroline. Their survey of the CSD suggested this to be a common attribute of such coordinated Hg centers.

These findings present a number of interesting questions that would have implications for spodium bonding in general. In the first place, is there something unique about the alkynyl group, and how might the spodium bonds respond to other substituents of differing electron-withdrawing capability? How might these conclusions be affected by replacing Hg by a lighter spodium atom with the same valence electron configuration such as Zn. It would be interesting as well to examine how these interactions are modulated by dialing up the nucleophilicity of the bases that approach this metal atom. What is the limit to the number of bases that might engage in a spodium bond with the central metal, and how does the spodium bond strength react to an increasing number of such bonds? From a more fundamental perspective, what is the full range of spodium bond strengths, and do they stray from the noncovalent domain to bonds that might be better described as coordinate covalent?

These questions are approached here from the perspective of quantum chemical calculations. A number of different systems are designed systematically to cover a wide range of both substituents on the spodium atom and attacking nucleophiles. Group 12 metal atoms are considered from both the top and bottom of the d-block of the periodic table. Specifically, Zn from the third period and Hg from the fifth period are expected to bracket and cover the full range of behavior of this group. Bases are added to the system one by one so as to determine how the presence of one affects the others, and to find the maximum number of such spodium bonds that each Lewis acid can sustain. These bonds are analyzed from several perspectives so as to establish the border beyond which a weak noncovalent bond passes into the realm of a stronger covalent bond.

METHODS

Quantum chemical calculations were carried out with the aid of the Gaussian 16[71] program. The M06-2X functional[72] was applied in the context of the def2-TZVP basis set which contains a triple-ζ foundation and a pseudopotential for Hg that includes some relativistic effects. This functional has been repeatedly assessed to be one of the most accurate for interactions such as those considered here.[73−80] Geometries were fully optimized, and verified as true minima by the lack of any imaginary vibrational frequencies. The interaction energy E_{int} is formulated as the difference between the energy of each complex and the sum of the energies of the two subunits in the geometry they adopt within the complex. E_{int} was corrected for basis set superposition error by the counterpoise procedure.[81] The Multiwfn program[82] located the extrema of the molecular electrostatic potential (MEP) on the ρ = 0.001 au isodensity surface of each monomer and provided the AIM analytical data.

Disubstituted MR_2 species considered include both Hg and Zn as Group 12 M atoms, from the first and third rows of transition metals of the periodic table so as to cover the full range of their behavior. The R substituents start with the C≡CH group so as to mimic the recent studies of alkynyl groups and their effect on spodium bonding.[70,83] The more electron-withdrawing C≡N group has also received some attention in the past[84] with which the calculated data can be compared. Finally, the more potent electron-withdrawing NO_2 was placed on the central spodium atom so as to examine an extreme in this regard. As Group 13 atoms such as Hg have a special affinity for N,[68] the bases considered to interact with the central spodium atom ranged from the weak NCH nucleophile with its sp hybridization of N, to the sp^3 NH_3 and NMe_3 whose electron-releasing methyl groups make it the most powerful nucleophile in this set.

RESULTS

Monomers. Each of the MR_2 monomers is fully linear in its configuration around the central M. It is surrounded by a molecular electrostatic potential (MEP) that features a belt of positive potential encircling the central M atom, as exemplified by $Hg(CN)_2$ and $Zn(CN)_2$ in Figure 1a,b, respectively. The magnitude of this band can be quantified as the maximum of the MEP on a 0.001 au isodensity surface, thought to roughly approximate a vdW surface. This quantity is defined as V_{max} and is presented in Table 1 for the six MR_2 monomers. These values are fairly large, and are substantially increased on reducing the size of the central M atom from Hg to Zn. There is also an enlarging effect as the R substituent varies from CCH to CN to NO_2.

Three different N-nucleophiles were allowed to interact with the MR_2 Lewis acid unit. The sp hybridization of the N in NCH makes it a fairly weak base, while NH_3 is stronger in this regard with its sp^3 hybridization. The replacement of the three H atoms by electron-donating Me groups makes NMe_3 the strongest nucleophile considered here.

Geometries. Some illustrative geometries adopted by the structures including one or more nucleophiles are displayed in Figures 2−4 for the Zn systems. (The coordinates of all complexes are contained in the Supporting Information.) The

https://doi.org/10.1021/acs.jpca.4c05481
J. Phys. Chem. A 2024, 128, 8751−8761

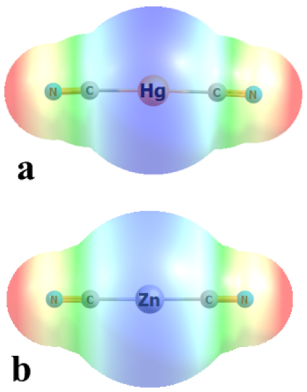

Figure 1. Molecular electrostatic potential (MEP) surrounding a) $Hg(CN)_2$ and b) $Zn(CN)_2$ on surface corresponding to 1.5× vdW radius. Red and blue regions respectively indicate negative and positive regions, ± 30 kcal/mol.

Table 1. Depth of π-Hole Surrounding M Atom of MR_2 Monomer, V_{max} in kcal/mol

M	CCH	CN	NO_2
Hg	24.7	51.5	50.9
Zn	38.2	70.3	76.4

first base settles into the positive region encircling the M atom. Note also that the addition of this base causes the ZnR_2 unit to bend from its monomer angle of 180°. This internal bend is not limited to only one base, but occurs for any number of nucleophiles, and the bend angle is designated as θ_0. Rather than locate opposite the first base, a second base instead takes up a position such that both bases lie in the plane perpendicular to the bent MR_2 molecule. The angle separating these two bases is defined as θ_1. When a third base can be accommodated by the system, all three bases occupy the same perpendicular plane. However, these bases are not equally separated, such that the θ_1 and θ_2 angles are generally different from one another, and from 120°.

The specific angles of the various complexes are collected in Tables 2 and 3 for the Hg and Zn systems, respectively. First with regard to the internal structure of the MR_2 units, HgR_2 suffers only a small amount of bending with θ_0 angles of 174° or higher when a single base is introduced. The bending is enhanced a bit as additional bases are added, as for example 161° for $Hg(NO_2)_2$ + 2 NMe_3. The degree of bending is much enhanced when Hg is replaced by Zn. The θ_0 angles are consistently below 160°, and some closer to 130°. The amount of bending corresponds to both the strength of the base, and its number.

Of perhaps greater interest is the disposition of the bases around the central MR_2 molecule. The bases can lie surprisingly close together. For example, the two NCH units lie only 66.6° apart when added to $Hg(CCH)_2$. This θ_1 angle describing their separation increases as the base grows stronger in the NCH < NH_3 < NMe_3 sequence. A similar angle increase arises as the R substituents become more electron-withdrawing. Comparison of Table 3 with 2 shows also that these separation angles are larger for Zn than for Hg.

In order to better understand the reason for the close positioning of the bases, as opposed to locations diametrically opposite to one another, the MEP of the complex containing a first base was analyzed. In the example of $Hg(CCH)_2$, association with a single NCH, resolves the full ring of positive potential of the monomer into a pair of equivalent and symmetric maxima, both making an angle of 90° with the N of the base, each of which can be considered a π-hole above the

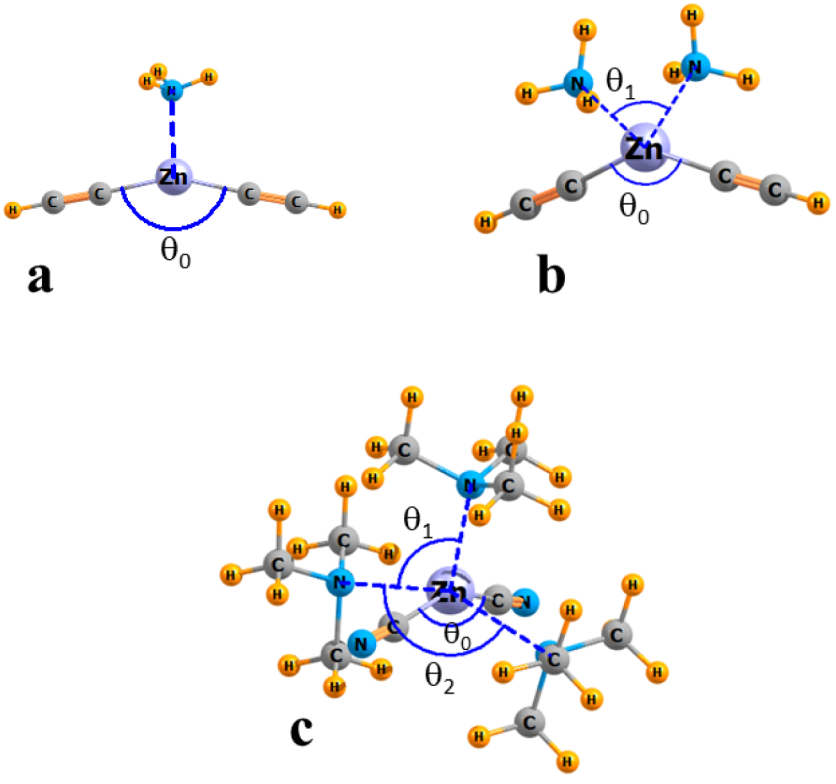

Figure 2. Molecular diagrams of $Zn(CCH)_2$ bound to a) 1, b) 2, and c) 4 nucleophiles, defining pertinent angles.

https://doi.org/10.1021/acs.jpca.4c05481
J. Phys. Chem. A 2024, 128, 8751−8761

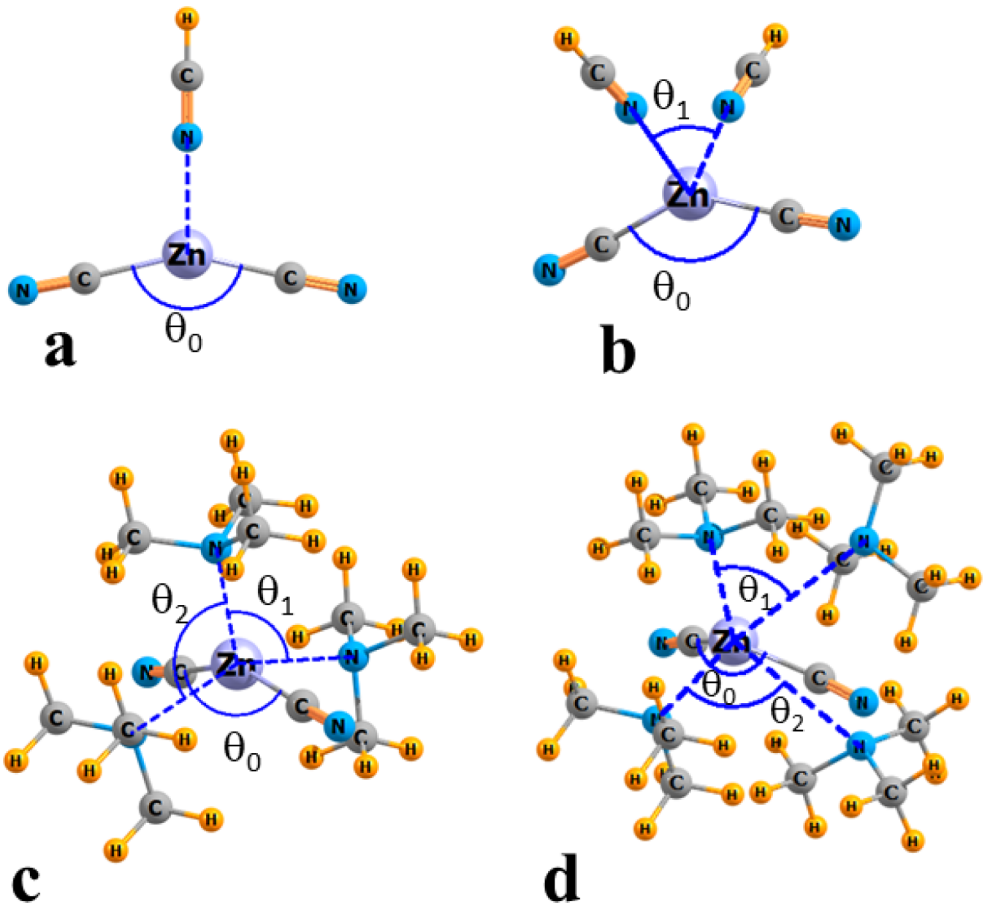

Figure 3. Molecular diagrams of $Zn(CN)_2$ bound to a) 1, b) 2, c) 3, and d) 4 nucleophiles, defining pertinent angles.

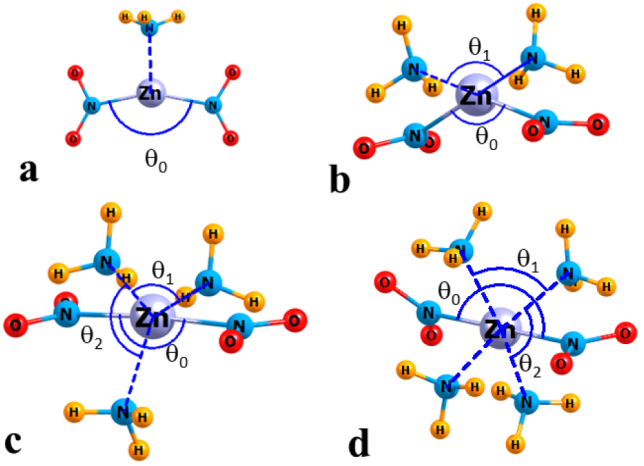

Figure 4. Molecular diagrams of $Zn(NO_2)_2$ bound to a) 1, b) 2, and c) 4 NH_3 nucleophiles, defining pertinent angles.

Hg. As another example, the angle between the N of NH_3 and the V_{max} of $Hg(CCH)_2$··NH_3 is also far less than 180°, at only 71°. One can conclude that the small angles between the first and second base in these complexes can be attributed at least in part to the perturbation that the first base exerts on the MEP of the central MR_2 unit.

The spodium bond lengths that stretch between the central M atom and each of the various N-bases are listed in Tables 4 and 5 for *M* = Hg and Zn, respectively. Several of the entries are blank, which indicates that the central MR_2 unit was unable to accommodate the indicated number of bases. For example, both $M(CCH)_2$ and $M(CN)_2$ are limited to no more than 2 NCH or NH_3 bases. There are several trends that are readily apparent from these tables. In the first place, these distances get progressively shorter as the weak nucleophile is replaced by NH_3 and then by NMe_3. The same contraction occurs as the R substituents of MR_2 are altered to more electron-withdrawing agents: CCH < CN < NO_2. As the number of surrounding nucleophiles *n* is increased, their distances from the M center likewise lengthen. Perhaps the most dramatic pattern is the much shorter M··N distances for Zn as compared to Hg. Taking the $M(CN)_2$ complex with NH_3 as an example, R (Zn··N) is equal to 2.154 Å, as compared to 2.696 Å for the Hg analogue. To be sure, some of this compression can be attributed to the smaller vdW radius of Zn, 2.39 Å as compared to 2.45 Å for Hg. But this difference of 0.06 Å is far less than the 0.55 Å shortening of R(M··N).

Energetics. These shorter spodium bond distances are suggestive of stronger bonds. This supposition is confirmed by the interaction energies contained in Tables 6 and 7 which refer to the interaction between the central MR_2 and the collection of *n* bases. For example, the interaction energy between $Hg(CCH)_2$ and a single NCH is 3.37 kcal/mol, which is nearly doubled for a pair of such bases. But this ratio is not characteristic of all these complexes: the average interaction energy of E_{int}/n does not necessarily diminish as *n* grows larger. For example, adding a second NMe_3 unit to $Hg(NO_2)_2$··NMe_3 raises this average from 20.6 to 22.3 kcal/mol. It should be emphasized at this point that due to the

https://doi.org/10.1021/acs.jpca.4c05481
J. Phys. Chem. A 2024, 128, 8751−8761

Table 2. Angles (degs) within Complexes Involving HgR_2

	1	2	3	4
$Hg(CCH)_2$	θ_0	θ_0, θ_1	θ_0, θ_1, θ_2	θ_0, θ_1, θ_2, θ_3
NCH	177.1	178.1	-	-
		66.6		
NH_3	175.8	173.6	-	-
		85.1		
NMe_3	175.8	173.5	176.3	173.2
		94.6	97.6	93.4
			99.1	75.1
				76.3
$Hg(CN)_2$				
NCH	176.4	176.4	-	-
		74.6		
NH_3	174.5	171.7	-	-
		87.3		
NMe_3	174.6	171.2	173.3	171.4
		98.1	101.6	76.8
			103.6	95.2
				111.2
$Hg(NO_2)_2$				
NCH	177.6	173.3	173.7	178.2
		78.8	77.2	79.0
			77.2	79.2
				119.8
NH_3	176.0	168.1	163.9	179.5
		111.3	97.0	92.2
			122.8	92.2
				92.2
NMe_3	173.5	161.1	165.4	-
		103.7	113.9	
			121.7	

Table 3. Angles (degs) within Complexes Involving ZnR_2

	1	2	3	4
$Zn(CCH)_2$	θ_0	θ_0, θ_1	θ_0, θ_1, θ_2	θ_0, θ_1, θ_2, θ_3
NCH	158.0	147.4	-	-
		88.7		
NH_3	154.2	142.7	-	-
		102.6		
NMe_3	152.3	140.5	149.6	-
		107.5	96.5	
			102.7	
$Zn(CN)_2$				
NCH	153.4	142.5	-	-
		93.5		
NH_3	150.9	139.8	-	-
		104.7		
NMe_3	149.8	138.0	153.4	139.0
		110.6	103.6	65.7
			103.6	78.4
				108.9
$Zn(NO_2)_2$				
NCH	-	133.7	131.8	180.0
		109.7	95.4	90.0
			131.8	90.0
				90.0
NH_3	153.6	136.8	175.7	180.0
		141.6	97.5	87.0
			129.2	87.1
				94.0
NMe_3	-	131.6	165.0	-
		116.9	111.7	
			102.9	

manner in which the interaction energy is calculated, any forces, whether attractive or repulsive, between the ligands themselves, will have little to no bearing on the interaction energy between the central MR_2 unit and its constellation of n surrounding ligands. However, it should also be understood that interligand interactions may have an influence on the geometries of certain multiligand structures. For example, a C··N tetrel bond between the two NCH ligands in $Hg(CCH)_2$··2NCH probably contributes to the small θ_1 angle in this complex.

Regarding the influence of base, metal, and substituent on the bond strengths, the trends largely mirror the bond distances in Tables 4 and 5. Zn forms much stronger bonds than does Hg, by a factor between 2 and 4. This bond energy is also enlarged in the NCH < NH_3 < NMe_3 sequence, in concert with the shorter distances. And the rising electron-withdrawing capacity of the R substituent is mirrored by the bond strengthening CCH < CN < NO_2. These bond energy patterns largely reproduce the π-hole depths of the MR_2 monomers exhibited in Table 1.

Analysis of the electron density topology via AIM reveals a bond path between the central M and the N atom of each base. The density at the bond critical point is compiled in Tables 8 and 9 for each complex and the patterns reinforce conclusions drawn on the basis of geometries and energetics. All of these densities are 0.04 au or below for the Hg systems in Table 8 which would place them in the noncovalent category. The Zn parallels are larger, between 0.04 and 0.07 au, so a certain degree of covalent character can be associated with them, particularly those on the high end of this spectrum. Like the geometrical and energetic markers, ρ_{BCP} reiterates the bond strengthening occurring as the substituent becomes more electron-withdrawing, and as the base itself becomes more potent. These densities are unambiguous as to the negative cooperativity as the number of surrounding bases increases, becoming smaller as one reads from left to right in these tables.

It is commonly thought that the sign of the total energy density H is an indicator of bond type, in that negative values signal a significant covalent component. These quantities are collected in Tables S1 and S2 for the Hg and Zn dyads, respectively, and confirm the conclusions from the bond critical point densities, as well as energetic and geometric aspects. The interactions between Hg and NCH lead to positive values of H, albeit small ones. These quantities turn negative for the stronger NH_3 and NMe_3 bases, more so as the R substituents become more electron-withdrawing. The most negative H quantities are −0.004 au for the $Hg(NO_2)_2$··$(NMe_3)_n$ systems. This pattern nicely coincides with the ρ_{BCP} values in Table 8 which exceed 0.04 au for the same set of complexes, and with average interaction energies of 20 kcal/mol, so are at least partially covalent.

Transition from Hg to Zn leads to similar trends in that H becomes more negative with stronger nucleophiles and more electron-withdrawing substituents. The principal difference lies in the magnitudes which are much larger for Zn. For example, H is negative even for the $Zn(CCH)_2$··$(NCH)_n$ systems, and becomes even more so for the more strongly bound complexes. The most negative values again arise for the $Zn(NO_2)_2$··$(NMe_3)_n$ systems, which can exceed −0.013 au. In concert

https://doi.org/10.1021/acs.jpca.4c05481
J. Phys. Chem. A 2024, 128, 8751−8761

Table 4. Spodium Bond Lengths from Central Hg to N of the Nucleophiles (R, Å)

	1	2	3	4
$Hg(CCH)_2$				
NCH	2.982	3.237	-	-
		3.304		
NH_3	2.805	2.817	-	-
		2.819		
NMe_3	2.752	2.753	2.773	-
		2.753	2.902	
			2.903	
$Hg(CN)_2$				
NCH	2.836	2.868	-	-
		2.903		
NH_3	2.696	2.706	-	-
		2.707		
NMe_3	2.642	2.648	2.676	2.722
		2.648	2.766	2.951
			2.862	3.296
				3.303
$Hg(NO_2)_2$				
NCH	2.732	2.740	2.733	2.782
		2.740	2.790	2.782
			2.791	2.810
				2.810
NH_3	2.567	2.551	2.492	2.546
		2.551	2.543	2.546
			2.572	2.547
				2.548
NMe_3	2.570	2.540	2.543	-
		2.540	2.545	
			2.654	

Table 5. Spodium Bond Lengths from Central Zn to N of the Nucleophiles (R, Å)

	1	2	3	4
$Zn(CCH)_2$				
NCH	2.282	2.278	-	-
		2.278		
NH_3	2.204	2.215	-	-
		2.215		
NMe_3	2.195	2.211	2.201	-
		2.211	2.372	
			2.859	
$Zn(CN)_2$				
NCH	2.179	2.194	-	-
		2.194		
NH_3	2.154	2.177	-	-
		2.177		
NMe_3	2.136	2.165	2.170	2.169
		2.165	2.460	2.248
			2.460	3.403
				3.959
$Zn(NO_2)_2$				
NCH	-	2.111	2.151	2.236
		2.111	2.235	2.236
			2.235	2.236
				2.236
NH_3	2.077	2.085	2.132	2.223
		2.085	2.133	2.223
			2.157	2.223
				2.223
NMe_3	-	2.114	2.140	-
		2.114	2.197	
			2.206	

with the BCP densities, interaction energies, and bondlengths, these bonds clearly contain a high degree of covalency.

DISCUSSION

The spodium bond between an atom of Group 12 and a N base covers a wide range. In the first place, the Zn atoms from the first transition state period form much stronger bonds than do the heavier Hg which lies two rows below Zn. One can attribute a qualitative difference as well, in that the bonds to Hg appear largely if not exclusively noncovalent, while the Zn··N bonds contain strong elements of covalency. The interaction energies for the Hg··N bonds lie in the span between 3.4 and 20.6 kcal/mol, as compared to the 12.2−43.9 kcal/mol range for Zn··N.

In geometrical terms, the Hg··N bondlengths span a range between 2.57 and 2.98 Å. While shorter than the sum of their vdW radii[85] of 4.11 Å, this range is much longer than the covalent radius sum[86] of 2.04 Å. The vdW and covalent radius sums for Zn··N are 4.05 and 1.89 Å, respectively. The corresponding Zn··N distances in the various complexes vary between 2.08 and 2.28 Å, only a little longer than the covalent sum. The stronger Zn··N spodium bonds also lend themselves to a much higher degree of bending of the RZnR molecule, in some cases to an angle less than 140°, whereas the smallest RHgR angle is 161°.

The AIM parameters echo this distinction between Hg··N and Zn··N bonds. While the bond critical point densities of the former are 0.04 au and below, it is only the weakest Zn··N bond with a density this small, some of them running all the way up to 0.07. As further confirmation, the total electron densities are either positive for the Hg systems or slightly negative. This behavior compares with the consistently negative energy densities for Zn··N which are appreciable in magnitude, as large as −0.013 au.

Table 6. Interaction Energies (kcal/mol) Between Central HgR_2 and the Collection of n Bases

	1	2	3	4
$Hg(CCH)_2$				
NCH	3.37	6.59	-	-
NH_3	7.71	16.31	-	-
NMe_3	10.61	21.99	28.08	
$Hg(CN)_2$				
NCH	7.74	14.55	-	-
NH_3	13.28	27.09	-	-
NMe_3	16.52	33.02	41.95	46.23
$Hg(NO_2)_2$				
NCH	9.27	19.76	29.25	37.71
NH_3	18.04	38.11	59.32	84.86
NMe_3	20.65	44.57	62.77	-

Whether Hg··N or Zn··N, the strengths of these bonds follow rules characteristic of noncovalent bonds. A more electron-withdrawing R substituent makes for a deeper π-hole around the central M, and a stronger M··N bond. A similar pattern is observed as the base becomes stronger from sp to sp.[3] It should also be noted that Zn has considerably deeper π-holes than do the Hg analogues, another factor contributing to the stronger Zn··N bonds.

https://doi.org/10.1021/acs.jpca.4c05481
J. Phys. Chem. A 2024, 128, 8751−8761

Table 7. Interaction Energies (kcal/mol) Between Central ZnR_2 and the Collection of n Bases

	1	2	3	4
$Zn(CCH)_2$				
NCH	12.23	27.13	-	-
NH_3	23.33	49.42	-	-
NMe_3	28.52	58.94	64.42	-
$Zn(CN)_2$				
NCH	21.51	43.36	-	-
NH_3	33.18	65.76	-	-
NMe_3	39.29	76.25	84.11	85.21
$Zn(NO_2)_2$				
NCH	[a]	56.64	74.49	85.25
NH_3	43.91	87.27	111.66	141.09
NMe_3	[a]	95.44	-	-

[a]NO_2 rearranges to Zn-ONO.

Table 8. Bond Critical Point Densities (au) on the Bond Path Connecting Hg with N of Base

	1	2	3	4
$Hg(CCH)_2$				
NCH	0.0153	0.0092	-	-
		0.0103		
NH_3	0.0252	0.0242	-	-
		0.0243		
NMe_3	0.0293	0.0289	0.0193	-
		0.0289	0.0240	
			0.0247	
$Hg(CN)_2$				
NCH	0.0206	0.0169	-	-
		0.0183		
NH_3	0.0315	0.0305	-	-
		0.0305		
NMe_3	0.0368	0.0359	0.0232	0.0111
		0.0359	0.0293	0.0239
			0.0344	0.0113
				0.0357
$Hg(NO_2)_2$				
NCH	0.0257	0.0242	0.0219	0.0212
		0.0242	0.0219	0.0212
			0.0244	0.0222
				0.0222
NH_3	0.0412	0.0421	0.0402	0.0421
		0.0421	0.0431	0.0422
			0.0469	0.0423
				0.0423
NMe_3	0.0428	0.0448	0.0359	-
		0.0449	0.0443	
			0.0445	

Regarding the maximum number of spodium bonds in which a given MR_2 molecule can participate, that number is 4, but can only be achieved in certain circumstances. Only two NCH or NH_3 nucleophiles can interact simultaneously with most of the MR_2 species. The exception occurs for the highly electron-withdrawing NO_2 substituent where M can host 4 of these bases, whether Hg or Zn. Although a stronger base, the large size of NMe_3 leads to steric problems. Three such bases can be accommodated by $M(CCH)_2$, and four by $M(CN)_2$. The bulkier NO_2 ligands limit the coordination of $M(NO_2)_2$ to only 3 NMe_3 ligands, despite the high strength of these bonds.

Table 9. Bond Critical Point Densities (au) on the Bond Path Connecting Zn with N of Base

	1	2	3	4
$Zn(CCH)_2$				
NCH	0.0403	0.0402	-	-
		0.0402		
NH_3	0.0533	0.0514	-	-
		0.0514		
NMe_3	0.0574	0.0547	0.0155	-
		0.0547	0.0391	
			0.0559	
$Zn(CN)_2$				
NCH	0.0514	0.0491	-	-
		0.0491		
NH_3	0.0602	0.0564	-	-
		0.0569		
NMe_3	0.0661	0.0611	0.0332	0.0062
		0.0611	0.0332	0.0302
			0.0603	0.0511
				0.0606
$Zn(NO_2)_2$				
NCH	0.0603	0.0585	0.0442	0.0438
		0.0585	0.0442	0.0438
			0.0526	0.0438
				0.0438
NH_3	0.0725	0.0704	0.0630	0.0514
		0.0704	0.0598	0.0514
			0.0636	0.0514
				0.0514
NMe_3	0.0729	0.0691	0.0433	-
		0.0691	0.0568	
			0.0576	

The placement of the *n* ligands around the central molecule is interesting. The first base bends the central RMR molecule and takes up its desired location along the R-M-R bisector. In doing so, it resolves the full π-hole ring encircling the linear monomer to a pair of π-hole points, lying very roughly 90° from the first ligand. As such, the second base is then attracted to this location, rather than to a site directly opposite the first ligand. Third and fourth bases follow similar guidelines, with all of the resulting N-M-N angles quite a bit less than 180°. The cooperativity between the bond strengths of multiple ligands is generally negative, with average interaction energies slightly less than the sum of *n* single bonds. But there are several exceptions where there is actually a small amount of positive reinforcement.

The recent literature is in accord with most of the conclusions reached here. Dicoordinated $HgCl_2$ was optimized in the presence of a set of molecules where Hg was allowed to interact with atoms of various sorts.[87] As in the work described above, these ligands introduced small nonlinearities into the $HgCl_2$ unit. Interaction energies were smallest for halogen, larger for chalcogen, and larger still for pnicogens. The value of 16.08 kcal/mol for NMe_3 compares well with our own 16.52 kcal/mol for $Hg(CN)_2\cdots NMe_3$. Energy decomposition of these complexes by Xia et al. placed the electrostatic term as the prominent contributor, followed by orbital interactions and then dispersion. To test whether this pattern is valid for the systems considered here, SAPT decomposition of the interaction between NMe_3 and both $Hg(CCH)_2$ and $Hg(CN)_2$ was carried out. Indeed, electrostatics accounted for slightly

https://doi.org/10.1021/acs.jpca.4c05481
J. Phys. Chem. A 2024, 128, 8751−8761

more than 50% of the total attractive energy, followed by dispersion and induction.

Another set of dicoordinated Hg systems[70] placed the Hg between a pair of alkynyl groups. The measured Hg··N distances when coordinated with the two N atoms of phenanthroline were 2.69 Å, similar to the bondlengths listed above for the complexes of $Hg(CCH)_2$ with a pair of NH_3 or NMe_3 bases. Survey of the CSD noted that Hg··N distances for pyridyl ligands typically lay between vdW and covalent radii sums, as computed here. Also confirmed was the greater bending of the Hg center as the interactions grew stronger. A similar complex, also involving phenanthroline, had been elucidated earlier within the solid state[88] with similar findings: R (Hg··N) = 2.68 Å. The Hg atoms within a similar scaffold with a pair of ethynyl ligands[83] engages in noncovalent interactions with the N atoms of pyridine with Hg··N distances of 2.73−2.80 Å; a slightly shorter distance of 2.64 Å emerged from another study,[89] all in the same range as the calculations here.

In crystals where $Hg(CN)_2$ is combined with a pair of N-ligands,[84] the N−Hg−N angles are less than 80°, and generally in the 79°-89° range for similar complexes, confirming the similarly small angles computed here. A comparable small angle of 95° was observed when the two nucleophilic atoms were S.[90] Earlier work[68,91] had confirmed the finding here that a disubstituted Hg is capable of engaging with four separate N atoms.

Tian et al.[26] had recently considered trisubstituted Hg with a pair of Cl substituents as well as a heterocyclic N. The spodium bonding of its π-hole to a series of bases containing chalcogen and pnicogen atoms, including NH_3, found the latter to be the most tightly bound, with an interaction energy of some 8.5 kcal/mol. As in the data computed here, the Hg··N distance lay between the vdW and covalent radii sum, closer to the latter.

In terms of higher coordination, Bauzá et al.[33] had noted that Cd had the deepest σ-hole in a set of tetrahedral tetracoordinated monomers, followed by Zn and then by Hg, with values in the 3−12 kcal/mol range. In complexes with a series of bases, the strongest were with N≡CMe, with interaction energies that remained quite similar down Group 12 but these values did not exceed 9 kcal/mol. Other calculations focused on Zn in a tetracoordinated framework,[31] finding interaction energies with N≡CMe and NMe_3 in the 7−12 kcal/mol range. Five-coordinated Zn within a porphyrin setting[32] interacts only weakly with NCH, with a binding energy of 2−4 kcal/mol.

The results described above of third-row Zn and fifth-row Hg are meant to cover the full range of Group 12 behavior. It is anticipated that fourth-row Cd will display properties intermediate between these two extremes. Indeed, an optimization of the geometry of the complex formed between $Cd(CCH)_2$ and NH_3 verified this supposition. The intermolecular M··N distance is 2.507 Å, intermediate between 2.805 Å for Hg and 2.204 Å for Zn. Likewise for the internal C-M-C angle of 165°, again between the extremes of 176° and 151°, respectively. As for the interaction energy, that for Cd is equal to 16.1 kcal/mol, as compared to 7.7 and 23.3 kcal/mol for Hg and Zn.

CONCLUSIONS

The linear MR_2 molecules contain a ring of positive potential encircling the central M atom. This π-ring is capable of attracting one or more nucleophiles to engage in a M··N spodium bond. It is possible for as many as four bases to approach the central molecule in this way under certain circumstances. The M··N spodium bond grows stronger as the nucleophilicity of the base and the electron-withdrawing power of the R substituent is enhanced. The interactions with Zn are far stronger than those with its heavier Hg congener. The weakest interaction energy between $Hg(CCH)_2$ and NCH is 3.4 kcal/mol, and the strongest involving $Zn(NO_2)_2$ and NH_3 as large as 44 kcal/mol. The total interaction between this same central molecule and four surrounding NH_3 bases is 141 kcal/mol. The bonds to Zn, particularly those with the sp^3 hybridized N-bases, contain an appreciable covalent component, with Zn··N distances barely longer than 2.0 Å, much shorter than Hg··N which lie in the range between 2.57 and 2.98 Å.

The bases position themselves directly above the R-M-R axis, and induce a certain amount of bending of the MR_2 molecule, particularly for Zn. In the case of multiple bases, they do not seek positions as removed from one another as possible. Rather, they tend to lie rather close together: some of the N··M··N angles are 90° or even less. There is a generally negative cooperativity between bond energies, but this is not always the case, as the average bond energy increases a small amount with n in certain cases.

It is to be stressed finally, that the calculations described above convey the full potential of these interactions if the various subunits are allowed to adopt their most favorable positions with respect to one another. In the case of an intramolecular spodium bond, the steric constraints attached thereto would likely induce a strain into each such bond, thereby weakening it. The same is true when placed within the context of a crystal, where a host of intermolecular interactions and crystal packing forces would generally restrain the constituents of the spodium bond from their optimal orientation, weakening it accordingly. Some of these same issues pertain to supramolecular assembly, where external considerations to achieve the optimal overall structure might override some of the natural proclivities of each of these spodium bonds, including the bending at the M center which differs from one metal atom to the next.

ASSOCIATED CONTENT

Supporting Information

The Supporting Information is available free of charge at https://pubs.acs.org/doi/10.1021/acs.jpca.4c05481.

Total energy density at bond critical points and coordinates of complexes (PDF)

AUTHOR INFORMATION

Corresponding Author

Steve Scheiner − *Department of Chemistry and Biochemistry, Utah State University Logan, Logan, Utah 84322-0300, United States;* orcid.org/0000-0003-0793-0369; Email: steve.scheiner@usu.edu

Author

Akhtam Amonov − *Department of Optics and Spectroscopy, Institute of Engineering Physics Samarkand State University, Samarkand 140104, Uzbekistan*

Complete contact information is available at: https://pubs.acs.org/10.1021/acs.jpca.4c05481

Notes

The authors declare no competing financial interest.

■ ACKNOWLEDGMENTS

This material is based upon work supported by the National Science Foundation under Grant No. 1954310.

■ REFERENCES

(1) Cuma, M.; Scheiner, S.; Kar, T. Effect of adjoining aromatic ring upon excited state proton transfer. o-Hydroxybenzaldehyde. *J. Mol. Struct.* **1999**, *467*, 37−49.
(2) Vinogradov, S. N.; Linnell, R. H. *Hydrogen Bonding*; Van Nostrand-Reinhold: New York, 1971.
(3) Joesten, M. D.; Schaad, L. J. *Hydrogen Bonding*; Marcel Dekker: New York, 1974; p 622.
(4) Arunan, E.; Desiraju, G. R.; Klein, R. A.; Sadlej, J.; Scheiner, S.; Alkorta, I.; Clary, D. C.; Crabtree, R. H.; Dannenberg, J. J.; Hobza, P. Definition of the Hydrogen Bond. *Pure Appl. Chem.* **2011**, *83*, 1637−1641.
(5) Grabowski, S. J. *Hydrogen Bonding - New Insights*; Springer: Dordrecht, Netherlands, 2006.
(6) Scheiner, S.; Wang, L. Hydrogen bonding and proton transfers of the amide group. *J. Am. Chem. Soc.* **1993**, *115*, 1958−1963.
(7) Scheiner, S.; Kleier, D. A.; Lipscomb, W. N. Molecular orbital studies of enzyme activity: I: Charge relay system and tetrahedral intermediate in acylation of serine proteinases. *Proc. Nat. Acad. Sci. U. S. A.* **1975**, *72*, 2606−2610.
(8) Cybulski, S.; Scheiner, S. Hydrogen bonding and proton transfers involving triply bonded atoms. HC≡N and HC≡CH. *J. Am. Chem. Soc.* **1987**, *109*, 4199−4206.
(9) Biswal, H. S.; Wategaonkar, S. OH···X (X = O, S) hydrogen bonding in thetrahydrofuran and tetrahydrothiophene. *J. Chem. Phys.* **2011**, *135* (13), 134306.
(10) Del Bene, J. E.; Alkorta, I.; Sanchez-Sanz, G.; Elguero, J. Structures, energies, bonding, and NMR properties of pnicogen complexes H_2XP: NXH_2 (X = H, CH_3, NH_2, OH, F, Cl). *J. Phys. Chem. A* **2011**, *115*, 13724−13731.
(11) Scheiner, S.; Lu, J. Halogen, Chalcogen, and Pnicogen Bonding Involving Hypervalent Atoms. *Chem.-Eur. J.* **2018**, *24*, 8167−8177.
(12) Bauzá, A.; Quiñonero, D.; Frontera, A.; Deyà, P. M. Substituent effects in halogen bonding complexes between aromatic donors and acceptors: A comprehensive ab initio study. *Phys. Chem. Chem. Phys.* **2011**, *13*, 20371−20379.
(13) Dong, W.; Li, Q.; Scheiner, S. Comparative Strengths of Tetrel, Pnicogen, Chalcogen, and Halogen Bonds and Contributing Factors. *Molecules* **2018**, *23*, 1681.
(14) Bauzá, A.; Mooibroek, T. J.; Frontera, A. Tetrel-Bonding Interaction: Rediscovered Supramolecular Force? *Angew. Chem., Int. Ed.* **2013**, *52*, 12317−12321.
(15) Grabowski, S. J. Halogen bond and its counterparts: Bent's rule explains the formation of nonbonding interactions. *J. Phys. Chem. A* **2011**, *115*, 12340−12347.
(16) Grabowski, S. J. Tetrel bond−σ-hole bond as a preliminary stage of the S_N reaction. *Phys. Chem. Chem. Phys.* **2014**, *16*, 1824−1834.
(17) Shields, Z. P.; Murray, J. S.; Politzer, P. Directional tendencies of halogen and hydrogen bonds. *Int. J. Quantum Chem.* **2010**, *110*, 2823−2832.
(18) Jovanovic, D.; Poliyodath Mohanan, M.; Huber, S. M. Halogen, Chalcogen, Pnictogen, and Tetrel Bonding in Non-Covalent Organocatalysis: An Update. *Angew. Chem., Int. Ed.* **2024**, *63*, No. e202404823.
(19) Zhang, Q.; Chan, Y.-Y.; Zhang, M.; Yeung, Y.-Y.; Ke, Z. Hypervalent Chalcogenonium···π Bonding Catalysis. *Angew. Chem., Int. Ed.* **2022**, *61*, No. e202208009.
(20) Lu, Y.; Liu, Q.; Wang, Z.-X.; Chen, X.-Y. Alkynyl Sulfonium Salts Can Be Employed as Chalcogen-Bonding Catalysts and Generate Alkynyl Radicals under Blue-Light Irradiation. *Angew. Chem., Int. Ed.* **2022**, *61* (16), No. e202116071.
(21) Hein, R.; Docker, A.; Davis, J. J.; Beer, P. D. Redox-Switchable Chalcogen Bonding for Anion Recognition and Sensing. *J. Am. Chem. Soc.* **2022**, *144*, 8827−8836.
(22) Docker, A.; Shang, X.; Yuan, D.; Kuhn, H.; Zhang, Z.; Davis, J. J.; Beer, P. D.; Langton, M. J. Halogen Bonding Tetraphenylethene Anion Receptors: Anion-Induced Emissive Aggregates and Photoswitchable Recognition. *Angew. Chem., Int. Ed.* **2021**, *60*, 19442−19450.
(23) Zhang, J.; Hao, A.; Xing, P. Hypervalent Iodine(III) Mediated Halogen Bonded Supramolecular Chiral System with Cholesteryl Naphthalimides. *Chem. -Eur. J.* **2024**, *30*, No. e202401004.
(24) Wang, Z.; Cao, Z.; Hao, A.; Xing, P. Pnictogen bonding in imide derivatives for chiral folding and self-assembly. *Chem. Sci.* **2024**, *15*, 6924−6933.
(25) Streit, T.-N.; Gomila, R. M.; Sievers, R.; Frontera, A.; Malischewski, M. CF_3-substituted sulfonium cations as efficient chalcogen bond donors towards cyanometalates. *CrystEngcomm* **2024**, *26*, 594−598.
(26) Tian, R.; Zeng, Y.; Li, X.; Zhang, X. The nature of π-hole spodium bonds in the $HgLCl_2$(L = pyrrole, pyrazole, imidazole, pyridine, pyridazine, and pyrimidine) complexes: From noncovalent to covalent interactions. *New J. Chem.* **2024**, *48*, 6582−6589.
(27) Gomila, R. M.; Tiekink, E. R. T.; Frontera, A. A Computational Chemistry Investigation of the Influence of Steric Bulk of Dithiocarbamato-Bound Organic Substituents upon Spodium Bonding in Three Homoleptic Mercury(II) Bis(N,N-dialkyldithiocarbamato) Compounds for Alkyl = Ethyl, Isobutyl, and Cyclohexyl. *Inorganics* **2023**, *11*, 468.
(28) Middya, P.; Karmakar, M.; Gomila, R. M.; Drew, M. G. B.; Frontera, A.; Chattopadhyay, S. The importance of spodium bonds, H-bonds and π-stacking interactions in the solid state structures of four zinc complexes with tetradentate secondary diamine ligands. *New J. Chem.* **2023**, *47*, 9346−9363.
(29) Yang, Q.; Wu, Q.; Zhang, X.; Yang, X.; Li, Q. Hydrogen and halogen bonds formed by MCO_3 (M = Zn, Cd) and their enhancement by a spodium bond. *Mol. Phys.* **2022**, *120*, No. e2102548.
(30) Jabłoński, M. Study of Beryllium, Magnesium, and Spodium Bonds to Carbenes and Carbodiphosphoranes. *Molecules* **2021**, *26*, 2275.
(31) Llull, R.; Montalbán, G.; Vidal, I.; Gomila, R. M.; Bauzá, A.; Frontera, A. Theoretical study of spodium bonding in the active site of three Zn-proteins and several model systems. *Phys. Chem. Chem. Phys.* **2021**, *23*, 16888−16896.
(32) Gomila, R. M.; Bauzá, A.; Mooibroek, T. J.; Frontera, A. Spodium bonding in five coordinated Zn(ii): A new player in crystal engineering? *CrystEngcomm* **2021**, *23*, 3084−3093.
(33) Bauzá, A.; Alkorta, I.; Elguero, J.; Mooibroek, T. J.; Frontera, A. Spodium Bonds: Noncovalent Interactions Involving Group 12 Elements. *Angew. Chem., Int. Ed.* **2020**, *59*, 17482−17487.
(34) Burguera, S.; Bauzá, A.; Frontera, A. A novel approach for estimating the strength of argentophilic and aurophilic interactions using QTAIM parameters. *Phys. Chem. Chem. Phys.* **2024**, *26*, 16550−16560.
(35) Yan, J.; Zeng, Y.; Meng, L.; Li, X.; Zhang, X. Gold(III) derivatives as the noncovalent interaction donors: Theoretical study of the π-hole regium bonds. *Phys. Chem. Chem. Phys.* **2023**, *25*, 29155−29164.
(36) Li, J.; Feng, Q.; Wang, C.; Mo, Y. On the nature of inter-anion coinage bonds. *Phys. Chem. Chem. Phys.* **2023**, *25*, 15371−15381.
(37) de las Nieves Piña, M.; Mooibroek, T. J.; Frontera, A.; Bauzá, A. Importance of Cu and Ag regium−π bonds in supramolecular chemistry and biology: A combined crystallographic and ab initio study. *Phys. Chem. Chem. Phys.* **2022**, *24*, 24983−24991.
(38) Pizzi, A.; Calabrese, M.; Daolio, A.; Ursini, M.; Frontera, A.; Resnati, G. Expanding the toolbox of the coinage bond: Adducts

https://doi.org/10.1021/acs.jpca.4c05481
J. Phys. Chem. A 2024, 128, 8751−8761

involving new gold(iii) derivatives and bioactive molecules. *CrystEngcomm* **2022**, *24*, 3846−3851.
(39) Shan, A.; Li, X.; Zeng, Y.; Meng, L.; Zhang, X. Theoretical investigation on the nature of substituted benzene···AuX interactions: Covalent or noncovalent? *New J. Chem.* **2022**, *46*, 3315−3324.
(40) Sánchez-Sanz, G.; Trujillo, C.; Alkorta, I.; Elguero, J. Rivalry between Regium and Hydrogen Bonds Established within Diatomic Coinage Molecules and Lewis Acids/Bases. *ChemPhyschem* **2020**, *21*, 2557−2563.
(41) Wang, R.; Wang, Z.; Yu, X.; Li, Q. Synergistic and Diminutive Effects between Regium and Aerogen Bonds. *ChemPhyschem* **2020**, *21*, 2426−2431.
(42) Daolio, A.; Pizzi, A.; Calabrese, M.; Terraneo, G.; Bordignon, S.; Frontera, A.; Resnati, G. Molecular Electrostatic Potential and Noncovalent Interactions in Derivatives of Group 8 Elements. *Angew. Chem., Int. Ed.* **2021**, *60*, 20723−20727.
(43) Calabrese, M.; Pizzi, A.; Daolio, A.; Beccaria, R.; Lo Iacono, C.; Scheiner, S.; Resnati, G. Osme Bond: Geometric and Energetic Features in the Adducts between OsO4 and Lewis Bases. *Chem. -Eur. J.* **2024**, *30*, No. e202304240.
(44) Burguera, S.; Gomila, R. M.; Bauzá, A.; Frontera, A. Matere Bonds in Technetium Compounds: CSD Survey and Theoretical Considerations. *Crystals* **2023**, *13*, 187.
(45) Burguera, S.; Sahu, A. K.; Chávez Romero, M. J.; Biswal, H. S.; Bauzá, A. Manganese matere bonds in biological systems: PDB inspection and DFT calculations. *Phys. Chem. Chem. Phys.* **2024**, *26*, 18606−18613.
(46) Grödler, D.; Burguera, S.; Frontera, A.; Strub, E. Investigating Recurrent Matere Bonds in Pertechnetate Compounds. *Chem. -Eur. J.* **2024**, *30*, No. e202400100.
(47) Xu, Y.; Calabrese, M.; Demitri, N.; Pizzi, A.; Nag, T.; Hung, I.; Gan, Z.; Resnati, G.; Bryce, D. L. Non-covalent matere bonds in perrhenates probed via ultrahigh field rhenium-185/187 NMR and zero-field NQR spectroscopy. *Chem. Commun.* **2023**, *59*, 12609−12612.
(48) Alkorta, I.; Elguero, J.; Frontera, A. Not Only Hydrogen Bonds: Other Noncovalent Interactions. *Crystals* **2020**, *10*, 180.
(49) Bauzá, A.; Frontera, A. Noncovalent Interactions Involving Group 6 in Biological Systems: The Case of Molybdopterin and Tungstopterin Cofactors. *Chem. -Eur. J.* **2022**, *28*, No. e202201660.
(50) Michalczyk, M.; Zierkiewicz, W.; Scheiner, S. Wolfium bonds in homodimers of MX_4Y (M = Mo, W; X = F, Cl, Br; Y = O, S, Se). *Phys. Chem. Chem. Phys.* **2024**, *26*, 5836−5847.
(51) Calabrese, M.; Gomila, R. M.; Pizzi, A.; Frontera, A.; Resnati, G. Erythronium Bonds: Noncovalent Interactions Involving Group 5 Elements as Electron-Density Acceptors**. *Chem. -Eur. J.* **2023**, *29*, No. e202302176.
(52) Mahmoudi, G.; Lawrence, S. E.; Cisterna, J.; Cárdenas, A.; Brito, I.; Frontera, A.; Safin, D. A. A new spodium bond driven coordination polymer constructed from mercury(ii) azide and 1,2-bis(pyridin-2-ylmethylene)hydrazine. *New J. Chem.* **2020**, *44*, 21100−21107.
(53) Burguera, S.; Bauzá, A.; Frontera, A. Hg(II)· d 8 [M] Interactions: Are they Metallophilic Interactions or Spodium Bonds? *ChemPhyschem* **2023**, *24*, No. e202300585.
(54) Kumar, P.; Frontera, A.; Pandey, S. K. Coordination versus spodium bonds in dinuclear Zn(ii) and Cd(ii) complexes with a dithiophosphate ligand. *New J. Chem.* **2021**, *45*, 19402−19415.
(55) Liu, N.; Li, Q. Group 12 Carbonates and their Binary Complexes with Nitrogen Bases and FH_2Z Molecules (Z = P, As, Sb): Synergism in Forming Ternary Complexes. *ChemPhyschem* **2021**, *22*, 1698−1705.
(56) Liu, N.; Xie, X.; Li, Q. Chalcogen Bond Involving Zinc(II)/Cadmium(II) Carbonate and Its Enhancement by Spodium Bond. *Molecules* **2021**, *26*, 6443.
(57) Liu, N.; Li, Q.; Scheiner, S. Spodium and tetrel bonds involving Zn(II)/Cd(II) and their interplay. *Chem. Phys.* **2022**, *556*, 111470.
(58) Wu, Q.; McDowell, S. A. C.; Li, Q. Single-electron spodium bonds: Substituent effects. *Appl. Organomet. Chem.* **2023**, *37*, No. e7052.
(59) Wysokiński, R.; Zierkiewicz, W.; Michalczyk, M.; Scheiner, S. Crystallographic and Theoretical Evidences of Anion···Anion Interaction. *ChemPhyschem* **2021**, *22*, 818−821.
(60) Biswal, H. S.; Kumar Sahu, A.; Frontera, A.; Bauzá, A. Spodium Bonds in Biological Systems: Expanding the Role of Zn in Protein Structure and Function. *J. Chem. Infor. Model.* **2021**, *61*, 3945−3954.
(61) Jena, S.; Dutta, J.; Tulsiyan, K. D.; Sahu, A. K.; Choudhury, S. S.; Biswal, H. S. Noncovalent interactions in proteins and nucleic acids: Beyond hydrogen bonding and π-stacking. *Chem. Soc. Rev.* **2022**, *51*, 4261−4286.
(62) Yashmin, F.; Mazumder, L. J.; Sharma, P. K.; Guha, A. K. Spodium bonding with noble gas atoms. *Phys. Chem. Chem. Phys.* **2024**, *26*, 8115−8124.
(63) Karmakar, M.; Frontera, A.; Chattopadhyay, S.; Mooibroek, T. J.; Bauzá, A. Intramolecular Spodium Bonds in Zn(II) Complexes: Insights from Theory and Experiment. *Int. J. Mol. Sci.* **2020**, *21*, 7091.
(64) Majumdar, D.; Frontera, A.; Gomila, R. M.; Das, S.; Bankura, K. Synthesis, spectroscopic findings and crystal engineering of Pb(ii)−Salen coordination polymers, and supramolecular architectures engineered by σ-hole/spodium/tetrel bonds: A combined experimental and theoretical investigation. *RSC Adv.* **2022**, *12*, 6352−6363.
(65) Garazade, I. M.; Gurbanov, A. V.; Gomila, R. M.; Frontera, A.; Nunes, A. V. M.; Mahmudov, K. T.; Pombeiro, A. J. L. Spodium, halogen and hydrogen bonds in the reactivity of bis(2,4-bis-(trichloromethyl)-1,3,5-triazapentadienato)-Zn(ii). *New J. Chem.* **2023**, *47*, 15856−15861.
(66) Gomila, R. M.; Frontera, A.; Tiekink, E. R. T. Supramolecular aggregation featuring Hg···S secondary-bonding interactions in crystals of mercury(ii) species augmented by computational chemistry calculations. *CrystEngcomm* **2023**, *25*, 5262−5285.
(67) Basak, T.; Gomila, R. M.; Frontera, A.; Chattopadhyay, S. Differentiating intramolecular spodium bonds from coordination bonds in two polynuclear zinc(ii) Schiff base complexes. *CrystEngcomm* **2021**, *23*, 2703−2710.
(68) Nockemann, P.; Schulz, F.; Naumann, D.; Meyer, G. Bis(trifluoromethyl)mercury(II) Complexes with Purine and 3, 5-Dimethyl-4′-amino-triazole as Ligands $[Hg(CF_3)2(Pur)]_4$ and $[Hg(CF_3)_2(Dat)]_2$. Bis(trifluormethyl)quecksilber(II)-Komplexe mit Purin und 3, 5-Dimethyl-4′-amino-triazol als Liganden: $[Hg(CF_3)_2(Pur)]_4$ and $Hg(CF_3)_2(Dat)]_2$. *Z. Anorg. Allg. Chem.* **2005**, *631*, 649−653.
(69) Naumann, D.; Schulz, F. Strukturen von neuen Bis-(pentafluorophenyl)halogenomercuraten $[\{Hg(C_6F_5)_2\}3(\mu\text{-}X)]$—(X = Cl, Br, I). *Z. Anorg. Allg. Chem.* **2005**, *631*, 715−718.
(70) Onn, C. S.; Hill, A. F.; Ward, J. S. Spodium bonding in bis(alkynyl)mecurials. *Chem. Commun.* **2024**, *60*, 2552−2555.
(71) Frisch, M. J.; Trucks, G. W.; Schlegel, H. B.; Scuseria, G. E.; Robb, M. A.; Cheeseman, J. R.; Scalmani, G.; Barone, V.; Petersson, G. A.; Nakatsuji, H., et al. *Gaussian 16 Rev. C.01*; Gaussian, Inc. Wallingford, CT, 2016.
(72) Zhao, Y.; Truhlar, D. G. The M06 suite of density functionals for main group thermochemistry, thermochemical kinetics, noncovalent interactions, excited states, and transition elements: Two new functionals and systematic testing of four M06-class functionals and 12 other functionals. *Theor. Chem. Acc.* **2008**, *120*, 215−241.
(73) Vamhindi, B. S. D. R.; Karton, A. Can DFT and ab initio methods adequately describe binding energies in strongly interacting $C_6X_6.C_2X_n$ $\pi-\pi$ complexes? *Chem. Phys.* **2017**, *493*, 12−19.
(74) Podeszwa, R.; Szalewicz, K. Communication: Density functional theory overcomes the failure of predicting intermolecular interaction energies. *J. Chem. Phys.* **2012**, *136*, 161102.
(75) Karthikeyan, S.; Ramanathan, V.; Mishra, B. K. Influence of the substituents on the CH···π interaction: Benzene−methane complex. *J. Phys. Chem. A* **2013**, *117*, 6687−6694.

https://doi.org/10.1021/acs.jpca.4c05481
J. Phys. Chem. A 2024, 128, 8751−8761

(76) Majumder, M.; Mishra, B. K.; Sathyamurthy, N. CH···π and π···π interaction in benzene-acetylene clusters. *Chem. Phys.* **2013**, *557*, 59−65.
(77) Vincent, M. A.; Hillier, I. H. The structure and interaction energies of the weak complexes of $CHClF_2$ and CHF_3 with HCCH: A test of denstiy functional theory methods. *Phys. Chem. Chem. Phys.* **2011**, *13*, 4388−4392.
(78) Boese, A. D. Density Functional Theory and Hydrogen Bonds: Are We There Yet? *ChemPhyschem* **2015**, *16*, 978−985.
(79) Walker, M.; Harvey, A. J. A.; Sen, A.; Dessent, C. E. H. Performance of M06, M06-2X, and M06-HF Density Functionals for Conformationally Flexible Anionic Clusters: M06 Functionals Perform Better than B3LYP for a Model System with Dispersion and Ionic Hydrogen-Bonding Interactions. *J. Phys. Chem. A* **2013**, *117*, 12590−12600.
(80) Molnar, L. F.; He, X.; Wang, B.; Merz, K. M. Further analysis and comparative study of intermolecular interactions using dimers from the S22 database. *J. Chem. Phys.* **2009**, *131* (6), 065102.
(81) Boys, S. F.; Bernardi, F. The calculation of small molecular interactions by the differences of separate total energies. Some procedures with reduced errors. *Mol. Phys.* **1970**, *19*, 553−566.
(82) Lu, T.; Chen, F. Multiwfn: A multifunctional wavefunction analyzer. *J. Comput. Chem.* **2012**, *33*, 580−592.
(83) Weisheim, E.; Weigel, S.; Neumann, B.; Stammler, H.-G.; Mitzel, N. W. Trifunctional organometallic frameworks and cages based on all-cis-1,3,5-triethynyl-1,3,5-trisilacyclohexanes. *Chem. Commun.* **2019**, *55*, 4985−4988.
(84) Cingolani, A.; Lorenzotti, A.; Gioia Lobbia, G.; Leonesi, D.; Bonati, F.; Bovio, B. Adducts from mercury(I) and mercury(II) compounds with Bispyrazolylalkanes.X-Ray crystal structure of Bis(3,5-dimethylpyrazol-l-yl)methane(dicyano)-mercury(II). *Inorg. Chim. Acta* **1987**, *132*, 167−176.
(85) Alvarez, S. A cartography of the van der Waals territories. *Dalton Trans.* **2013**, *42*, 8617−8636.
(86) Pyykkö, P.; Atsumi, M. Molecular Single-Bond Covalent Radii for Elements 1−118. *Chem. -Eur. J.* **2009**, *15*, 186−197.
(87) Xia, T.; Li, D.; Cheng, L. Theoretical analysis of the spodium bonds in $HgCl_2$···L (L = ClR, SR_2, and PR_3) dimers. *Chem. Phys.* **2020**, *539*, 110978.
(88) Gutiérrez-Puebla, E.; Vegas, A.; García-Blanco, S. The adduct bis(phenylethynyl)mercury-1,10-phenanthroline. *Acta Cryst. B* **1978**, *34*, 3382−3384.
(89) Hoskins, B. F.; Robson, R.; Sutherland, E. E. Bis(4-pyridylethynyl)mercury. *J. Organomet. Chem.* **1996**, *515*, 259−260.
(90) Altaf, M.; Stoeckli-Evans, H.; Ahmad, S.; Isab, A. A.; Al-Arfaj, A. R.; Malik, M. R.; Ali, S. Crystal Structure of a Trinuclear Mercury(II) Cyanide Complex of Tetramethylthiourea, [{(Tetramethylthiourea)-2Hg(CN)2}2·Hg(CN)2]. *J. Chem. Cryst.* **2010**, *40*, 1175−1179.
(91) Dewhurst, R. D.; Hill, A. F.; Willis, A. C. A mercury bis(tricarbido) complex: $[Hg\{C{=}C{-}C{=}W(CO)_2Tp\}_2(dmso)_4]$-$(dmso)_2$ (Tp = hydrotrispyrazolylborate). *Chem. Commun.* **2004**, 2826−2827.

https://doi.org/10.1021/acs.jpca.4c05481
J. Phys. Chem. A 2024, 128, 8751−8761